Improved Hole Repairing Method Based on Wavefront Method

Jing Huang (huangjing@139.com)
Beijing Normal University https://orcid.org/0000-0002-5990-8027
Weicong Li
Beijing Normal University
Mengjie Ye
Beijing Normal University

Research

Keywords: Wavefront method, Hole repairing, Triangle mesh, Curvature recovery

Posted Date: March 8th, 2022

DOI: https://doi.org/10.21203/rs.3.rs-1345779/v1

RESEARCH

Improved Hole Repairing Method Based on Wavefront Method

Jing Huang*, Weicong Li and Mengjie Ye

*Correspondence:
huangjing@139.com
Research Center for Intelligent Engineering and Educational Application, Beijing Normal University at Zhuhai, Zhuhai, China
Full list of author information is available at the end of the article

Abstract

Due to the emergence of 3D scanning technology, in the process of acquiring spatial information of the model, incomplete data often results in the loss of model data, which leads to holes in the acquired digital model. The defective model affects the appearance of the model. What's more, it will cause a lot of inconvenience to the subsequent research and treatments. Regarding the problems existing in the hole repairing of the 3D scanning model, a hole repairing method based on the improved wavefront method is proposed in this paper. After the initial mesh is formed by the wavefront method, the curvature can be repaired and the triangle patch can be rotated to a reasonable position. The experimental results show that the algorithm effectively and quickly generates high-quality closed meshes in the corresponding hole types. Besides, it can accurately restore the geometric features of the hole area while retaining the original information of the model. The proposed algorithm in this paper can be applied in the fields of reverse engineering, archaeology, digital heritage, medical visualization, 3D reconstruction, etc.

Keywords: Wavefront method; Hole repairing; Triangle mesh; Curvature recovery

1 Introduction

Continuous breakthroughs have been made in computer vision technology in recent years. 3D spatial scanning technology can convert the spatial 3D information of the object into digital signals that can be processed by the computer, which provides people with a very convenient means to digitize the 3D model of the object. 3D models are widely used in reverse engineering, finite element analysis, archaeology, digital heritage, medical visualization, automatic driving, virtual reality, biomedicine, 3D reconstruction, and other fields[1, 2, 3].

At the time of obtaining the spatial information of the model, the obtained data will be incomplete. There may be several reasons from many aspects explaining this. For example, when scanning a 3D target with a 3D laser scanner, the lost local information of the entity itself often leads to the loss of 3D scanning data information to further produce holes in the obtained digital model due to the complexity of the target object surface (depression, bending, etc.), the limitation of the visible field of view of the scanning equipment or the damaged or defective surface of the scanned object. The defective model affects the appearance of the model. What's more, it will cause a lot of inconvenience to the subsequent research and treatments. For example, in the research on the protection of cultural relics, the cultural relics that have passed through the years or have been affected to varying degrees are scanned

and repaired by the 3D geometric information with holes. Finally, a complete digital model is generated so that the digital cultural relics can be permanently preserved, which plays a very important role in the research, reproduction, relocation, and virtual exhibition of cultural relics[4, 5]. In the cranioplasty operation, we can scan the missing bones and repair the scanned model of missing holes before the operation to make a repairosome consistent with the bones, which not only shortens a lot of operation time but also reduces the operation risk. In the 3D reconstruction, if there are holes in the model, the results will be incorrect.

Domestic and foreign researchers have proposed a variety of classical 3D model hole repairing algorithms. Davis et al.[6] used the voxel to define a symbolic distance field and adopted diffusion operators to diffuse voxels to the hole area on the contour surface to repair the 3D model holes. However, its calculation efficiency was low and the repair results could not restore the characteristics of the original model. Ju[7] put forward the concept of the inner/outer body of voxel and established the octree mesh model. Then, the equidistant surface was extracted to reconstruct the surface. It is not only an effective method to repair arbitrary polygon 3D models but also is provided with robustness. However, the repair quality of the complex 3D model is also lower than that of the original model. Hétroy et al.[8]used voxels to represent the input arbitrary polygon mesh data and then converted the corrected voxels back to the mesh data. This algorithm has a good effect on the large-area hole repair but the repair effect is not ideal for the hole area that requires repairing detailed features.

Zhang et al.[9] first found two boundaries with the minimum included angle by traversing the model hole's boundary and directly connecting them to judge the location of the new points. However, the new triangle patches in this method have different sizes, strange shapes, and poor repair effects. Wang et al. [10] used the wavefront method to repair the holes to obtain the initial mesh and then adopted the spatial information of the boundary to calculate the reasonable position of the new points and adjust the position of the triangle patch of the initial mesh. This method can completely seal the repair hole but it will cause the loss of the geometric features with large curvature change. Besides, the repair effect is relatively flat. Ji et al.[11] used the principle of minimum angle to obtain the initial repair mesh of the hole and then established RBF (radial basis function) to fit the curved surface by adjusting the initial mesh to the fitting curved surface. The repair result of this method is relatively smooth but the triangle mesh will be deformed in the process of adjusting the normal direction of the triangle patch. At the same time, this method can only meet the local hole repair.

2 Methods

2.1 Wavefront method

The wavefront method is often used to quickly seal and fill holes in boundary pretreatment as a result of its good robustness and is deemed as a very important idea in hole repair of the mesh model. The wavefront method is equipped with the idea of recursion to quickly generate the repair mesh with good controllability[12]. The wavefront method is implemented based on triangulation. To obtain the optimal repair mesh at one time, the traditional triangulation is added with many

constraints when repairing holes, such as the dynamic programming algorithm with time complexity of as high as $O(n^3)$ used by Liepa[13].

The basic realization of the traditional wavefront method is to initialize the boundary set of holes connected from the head to the tail, which is called wavefront. The triangle mesh vertex sequence set is known as $\{V_i\}$ with a boundary V_i as the starting point to continuously generate triangles into the hole as shown in Figure 1. The wavefront is updated each time a triangle is generated, and the boundary gradually shrinks until the wavefront is empty. At the time of the use of the wavefront method, the boundary point with the minimum angle is selected as the starting point for repair. The specific implementation steps are as follows:

(1) Test the hole and obtain the set of boundary points of the hole to initialize the wavefront.

(2) Calculate the included angle formed by the half-edges of all adjacent boundaries on the hole boundary.

(3) Find the minimum included angle θ_{min} composed of boundary points and add a new triangle patch according to the rules of the new triangle starting from the corresponding half-edge. The rules are as follows: Assuming the thresholds of two angles as α and β $(0 < \alpha < \beta < \pi)$, when $0 < \theta_{min} \leq \alpha$, it is needed to connect two points V_{i-1} and V_{i+1} to form a new triangle surface. When $\alpha < \theta_{min} \leq \beta$, it is needed to add the new point V_{new} on the bisection direction of θ_{min} at the place where the length is the average length $l = (l_{V_{i-1}V_i} + l_{V_iV_{i+1}})/2$ obtained from the sum of both sides of $V_{i-1}V_i$ and V_iV_{i+1}, and then connect V_iV_{new}, $V_{new}V_{i-1}$and $V_{i+1}V_{new}$ to form two new triangle patches. When $\beta < \theta_{min} < \pi$, it is needed to add the new point V_{new1} and V_{new2} on the trisection direction of θ_{min} at the place where the length is the average length $l = (l_{V_{i-1}V_i} + l_{V_iV_{i+1}})/2$ obtained from the sum of both sides of $V_{i-1}V_i$ and V_iV_{i+1}, and connect V_iV_{new1}, $V_{new1}V_{i-1}$, V_iV_{new2}, $V_{new2}V_{new1}$, and $V_{i+1}V_{new2}$ in turn to form three new triangle patches.

(4) Add the newly added triangle patches to the triangle patch sequence of the wavefront.

(5) Repeat (2)-(4) until the hole is filled. When the number of boundary point is equal to 3, it is needed to stop adding new points. The hole repair is deemed as having been completed.

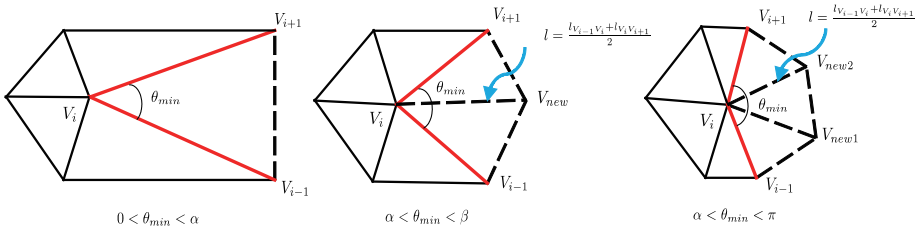

Figure 1 Rules of Adding A New Triangle by Traditional Wavefront Method

Because the traditional hole repair algorithm based on the wavefront method is provided with the minimum angle principle, the boundary point with the minimum included angle is repaired every time. In addition, the side length of the surface added each time by the wavefront method depends on the length of the adjacent

sides of the processing point, which will lead to the newly added triangle becoming smaller and smaller after repair. There may be situations where it is impossible to makeup or it takes a long time. Experiments show that in the actual hole repair process, for holes with large curved surface curvature, only one side of the hole is often repaired, which greatly prolongs the repair time while resulting in the different distribution of the mesh density, the poor shape effect and even the frequent occurrence of incomplete repair. As shown in Figure 2, (a) is a model with holes. After 2000 iterations of this hole, there is a tendency to focus on the treatment on one side as shown in the red circles in (b) and (c).

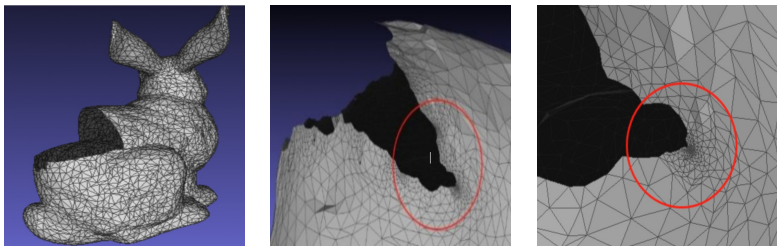

(a) (b) (c)

Figure 2 Disadvantages of Traditional Wavefront Method (a) Model with Holes; (b)Key Treatment on One Side of the Hole; (c) Zoom in to Observe the Part that Got the key Treatment on One Side of the Hole

2.2 Improvement Based on Traditional Wavefront Method

Lu[14] proposed an improvement on the traditional wavefront method after considering the generation of long and narrow triangle patches. However, a lot of calculations were increased. The minimum angle is almost impossible to be greater than, and only the concave angle can be considered. Besides, the length of each side of the added face is the same as the original rule, so it will still focus on repairing one side. The algorithm in the paper is improved based on the wavefront method proposed by Lohner et al. [15] and Lo [16]. When obtaining the processing point of the minimum angle, the judgment conditions are added as shown in Figure 3:

(1) Test the hole and obtain the hole boundary point set; calculate the average length $Avglen$ of the current hole boundary before the initialization of the wavefront.

(2) Calculate the included angle formed by half-edges of all adjacent boundaries on the hole boundary.

(3) If the included angle θ_{min} of this point is within $0 < \theta_{min} < \mu$ (The value of μ can be changed. The default value: $\mu = 150°$), the point with the smallest angle is still used as the treatment point to start the repair.

(4) If the included angle θ_{min} of this point is within $\mu \leq \theta_{min} \leq \pi$, it is needed to select a point randomly among all current boundary points as the processing point.

(5) Add a new triangle patch on the processing point according to the rule of adding a new triangle. The rules are as follows: assuming that the thresholds of two angles as α and β ($0 < \alpha < \beta < \pi$, $\alpha = 75°$, and $\beta = 135°$ by default). As shown in Figure 4, when $0 < \theta_{min} \leq \alpha$, the rule remains unchanged and it is needed to connect two points V_{i-1} and V_{i+1} to form a new triangle surface. When

$\alpha < \theta_{min} \leq \beta$, it is needed to add the new point V_{new} on the bisection direction of θ at the place where the length is $Avglen$ and connect V_iV_{new}, $V_{new}V_{i-1}$ and $V_{i+1}V_{new}$ in turn to form two new triangle patches. When $\beta < \theta < \pi$, it is needed to add the new point V_{new1} and V_{new2} on the trisection direction of θ at the place where the length is $Avglen$ and connect V_iV_{new1}, $V_{new1}V_{i-1}$, V_iV_{new2}, $V_{new2}V_{new1}$ and $V_{i+1}V_{new2}$in turn to form three new triangle patches.

(5) Add the newly added triangle patches to the wavefront.

(6) Repeat (2)-(5) until the hole is filled. When the number of boundary point is equal to 3, it is needed to stop adding new points. The remaining three boundary points form a triangle patch and the hole repair is deemed as has been completed.

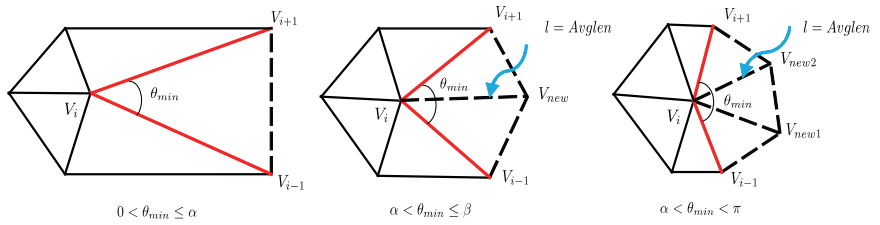

Figure 3 Rules of Adding A New Triangle by Improved Wavefront Method

2.2.1 Curvature restoration

There are many ways to realize the curvature restoration of the hole area. For example, Li et al. [17] established Poisson's equation to reconstruct the initialized mesh to fit the curved surface and then stitched the predicted surface with the original model. Liu et al. [18] weighted the corrected normal direction of the vertex of the hole vertices and then established a weighting function to solve the minimized weighting function. Later, the coordinates of the new points to adjust the curvature were obtained. Ji et al. [11] used the radial basis function to build implicit equations for curved surfaces and then mapped the newly added points onto the curved surface.

The hole region curvature restoration method used in the paper is to make use of the geometric space information of the boundary vertices to rotate the new triangle patches to a reasonable position so that the new triangle patches can fit the surface features of the original model as much as possible and realize the original geometric shape restoration of the missing part of the model. This method can restore the curvature quickly and effectively without increasing the computational pressure of the program.

An adjacent domain triangle surface of the boundary vertex V_i in the triangle mesh model is shown in Figure 4. V_{i-1}, V_i and V_{i+1} are the boundary points adjacent to the hole and f_k is a triangle patch of *1-ring*. $N_{f_k}$is the normal direction of f_k and g is the center of gravity of f_k. G_k is the distance from g to V_i and N_{V_i} is the expected normal direction of V_i.

The expected normal direction of a vertex is obtained by the weighted average of the normal directions of all its adjacent triangle patches. Assuming that vertex V_i has n adjacent surfaces and the weight of the triangle patch f_k is ω_k, the expected normal direction of the vertex is calculated by Equation (1).

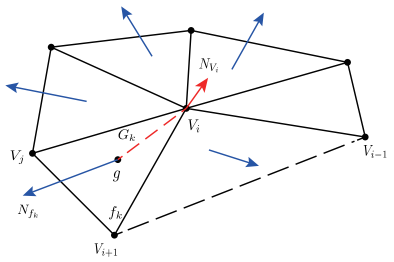

Figure 4 An Adjacent Domain Triangle Surface of the Boundary Vertex V_i

$$N_{v_i} = \sum_{k=1}^{n} \omega_i N_{f_i} \tag{1}$$

ω_k has a great influence on the calculated expected normal direction of the vertex. At present, there are many methods to calculate the weight and different parameters will be taken into account. The weight calculation Equation (2) used in the paper refers to the ratio of triangular shape factor λ to the distance V_i from the center of gravity to G_k proposed by Lu [14], the weight ω_k is defined as follows.

$$\omega_k = \lambda / G_k \tag{2}$$

Triangle shape factor refers to the value of twice the ratio of the radius of the inscribed circle to the radius of the circumscribed circle. Assuming that the lengths of the three sides of the triangle are a, b and c, and the area is S, the Equation (3) for calculating the shape factor λ is as follows according to the deduction from the Equation $r = 2S/(a+b+c)$of the radius of the inscribed circle and Equation $R = abc/4S$ of the radius of the circumscribed circle.

$$\lambda = 2 \times \left(\frac{2S/(a+b+c)}{abc/4S} \right) \tag{3}$$

According to Heron's formula $S = \sqrt{p(p-a)(p-b)(p-c)}$ and the application of the perimeter $p = (a+b+c)/2$ into Equation (3), the final Equation (4) of the shape factor can be obtained.

$$\lambda = \frac{(a+b-c)(a+c-b)(b+c-a)}{abc} \tag{4}$$

As shown in Figure 4, V_iV_{i+1} and V_iV_{i-1} are the boundary edges of holes. When calculating the expected normal direction of the vertex V_i, it is necessary to add the triangle patch $V_iV_{i+1}V_{i-1}$ into the equation, that is, to make up all adjacent triangles before calculating. The aim is to make the calculation result more complete.

According to the new rules of adding the new triangle patches, three different conditions correspond to different ways of estimation.

Case (a) is to add a new triangle patch $V_iV_{i+1}V_{i-1}$, then the expected normal direction of the triangle patch $V_iV_{i+1}V_{i-1}$ is the average value of the expected normal directions of the three vertices, that is $N'_f = (N_{V_i} + N_{V_{i+1}} + N_{V_{i-1}})/3$.

Case (b) is to add two new triangle patches $V_iV_{new}V_{i+1}$ and $V_iV_{i-1}V_{new}$, then the expected normal direction of the triangle patch $V_iV_{new}V_{i+1}$ is the average value of the expected normal directions V_i and V_{i+1}, that is, $N'_{f_1} = (N_{V_i} + N_{V_{i+1}})/2$. Similarly, the expected normal direction of the triangle patch $V_iV_{i-1}V_{new}$ is $N'_{f_2} = (N_{V_i} + N_{V_{i-1}})/2$.

Case (c) is to add three new triangle patches $V_iV_{new2}V_{i+1}$, $V_iV_{i-1}V_{new2}$ and $V_iV_{new1}V_{new2}$. Because the known geometry information of the triangle patch $V_iV_{new1}V_{new2}$ is less, the normal direction adjustment for the triangle patch is not performed. The adjustment only be performed for the triangle patches $V_iV_{new2}V_{i+1}$ and $V_iV_{i-1}V_{new2}$ and their expected normal directions are $N'_{f_1} = (N_{V_i} + N_{V_{i+1}})/2$ and $N'_{f_2} = (N_{V_i} + N_{V_{i-1}})/2$ respectively.

Assuming that the new triangle patch f is rotated, N_f is the original normal direction of f, N'_f is the expected normal direction of f, g is the center of gravity of f with a direction of rotation axis $N_{rotate} = N_f \times N'_f$, a rotation angle $\theta = \langle N_f, N'_f \rangle$. Because it rotates around the center of gravity and the rotation axis does not pass through the origin, it is necessary to translate the center of gravity to the origin to rotate and then translate back.

The rotation matrix R_{xyz} is as shown in Equation (5)

$$R_{xyz} = \begin{bmatrix} x^2 + \left(y^2 + z^2\right)\cos\theta & xy(1-\cos\theta) - z\sin\theta & xz(1-\cos\theta) + y\sin\theta \\ xy(1-\cos\theta) + z\sin\theta & y^2 + \left(x^2 + z^2\right)\cos\theta & yz(1-\cos\theta) - x\sin\theta \\ xz(1-\cos\theta) - y\sin\theta & yz(1-\cos\theta) + x\sin\theta & z^2 + \left(x^2 + y^2\right)\cos\theta \end{bmatrix} \quad (5)$$

The translation matrix T_{xyz} is as shown in Equation (6)

$$T_{xyz} = \begin{bmatrix} \left(a\left(y^2 + z^2\right) - x(by + cz)\right)(1 - \cos\theta) + (bz - cy)\sin\theta \\ \left(b\left(x^2 + z^2\right) - y(ax + cz)\right)(1 - \cos\theta) + (cx - az)\sin\theta \\ \left(c\left(x^2 + y^2\right) - z(ax + by)\right)(1 - \cos\theta) + (ay - bx)\sin\theta \end{bmatrix} \quad (6)$$

So, the final transformation matrix $M_{xyz} = R_{xyz}T_{xyz}$ is as shown in Equation (7):

$$M_{xyz} = \begin{bmatrix} R_{xyz} & T_{xyz} \\ \mathbf{0} & 1 \end{bmatrix} \quad (7)$$

In Equations (5), (6), and (7), θ is the rotation angle, and x, y, and z correspond to the coordinates of the rotation axis N_{rotate} respectively. a, b and c correspond to the coordinates of the center of gravity $g = (a, b, c)$ respectively.

After the triangle patch is processed by the above change matrix, the triangle patch can be rotated around its center of gravity to the new position behind the expected normal direction as shown in Figure 5.

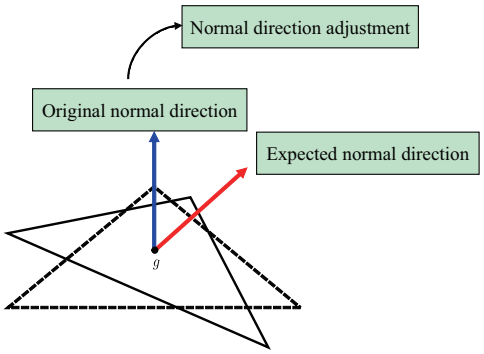

Figure 5 Schematic Diagram of Rotation of Triangle Patch

2.2.2 Hole repair process

The mesh model data is firstly input into the hole repairing process and then the improved wavefront method is used to repair the triangle patches of the holes. Meanwhile, the curvature of each triangle patch is repaired until all the holes are repaired. The repaired mesh model data is output as shown in the specific process of Figure 6.

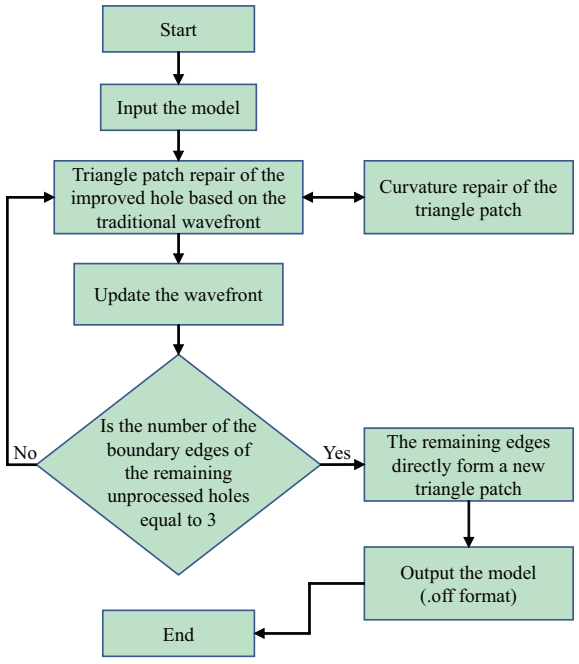

Figure 6 Hole Repair Process

3 Results and discussion

The proposed algorithm in this paper is implemented by C++ on a computer with an i7 processor, CPU with a basic frequency of 2.60GHz, and a memory of 16.0GB. Several models with holes are repaired below.

(1) Repair the bunny model with holes. Conditional thresholds are set to $\alpha = 75°$, $\beta = 135°$, $\mu = 150°$ respectively. The effect comparison of models before and after the repair is shown in Figure 7.

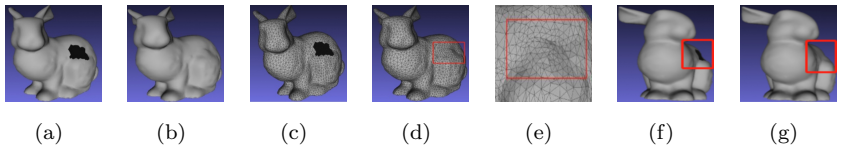

(a) (b) (c) (d) (e) (f) (g)

Figure 7 bunny Model (a)Render Model Before Repair; (b)Render Model After Repair; (c)Mesh Model Before Repair; (d)Mesh Model after Repair; (e)Repair Details; (f)Hole Observation; (g)Repair Effect Observation

(2) Repair the rocker model. Conditional thresholds are set to $\alpha = 95°$, $\beta = 135°$, $\mu = 150°$ respectively. The effect comparison of models before and after the repair is shown in Figure 8.

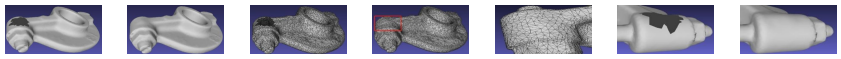

(a) (b) (c) (d) (e) (f) (g)

Figure 8 rocker Model (a)Render Model Before Repair; (b)Render Model After Repair; (c)Mesh Model Before Repair; (d)Mesh Model after Repair; (e)Repair Details; (f)Hole Observation; (g)Repair Effect Observation

(3) Repair the horse model. Conditional thresholds are set to $\alpha = 90°$, $\beta = 135°$, $\mu = 150°$ respectively. The effect comparison of models before and after the repair is shown in Figure 9.

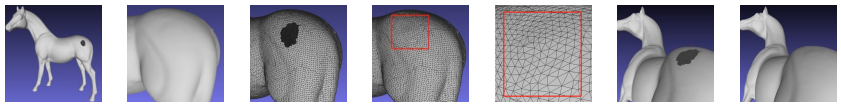

(a) (b) (c) (d) (e) (f) (g)

Figure 9 horse Model (a)Render Model Before Repair; (b)Render Model After Repair; (c)Mesh Model Before Repair; (d)Mesh Model after Repair; (e)Repair Details; (f)Hole Observation; (g)Repair Effect Observation

(4) Repair the blobby model. Conditional thresholds are set to $\alpha = 90°$, $\beta = 135°$, $\mu = 150°$ respectively. The effect comparison of models before and after the repair is shown in Figure 10.

The following table shows the data comparison before and after the repair of the hole model with the hole repair method based on the improved wavefront method.

3.1 Comparison of the algorithm of the paper and the effect of MeshLab software

MeshLab is deemed as a commonly used open-source software for processing and editing triangular mesh models. The software has the function of repairing holes in the triangle mesh models. The repair effect by using this function is compared with the algorithm effect in the paper as shown in Figures 11, 12, 13 and 14.

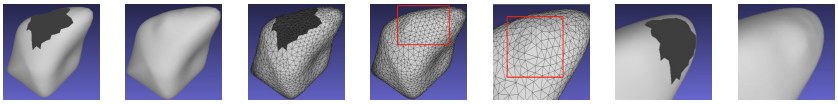

(a) (b) (c) (d) (e) (f) (g)

Figure 10 blobby Model (a)Render Model Before Repair; (b)Render Model After Repair; (c)Mesh Model Before Repair; (d)Mesh Model after Repair; (e)Repair Details; (f)Hole Observation; (g)Repair Effect Observation

Table 1 Data Comparison Before and After Repair of the Hole Model

Model name	Number of triangles (front)	Number of triangles (back)	Number of added triangles	Number of vertices (front)	Number of vertices (back)	Number of added vertices	Number of boundary edges	Running time (s)
bunny	8546	8720	174	4289	4365	76	36	3.2360
rocker	18686	18686	120	9359	9359	43	34	5.307
horse	96764	96980	216	48403	48492	89	40	21.769
blobby	3854	4072	218	1948	2038	90	40	2.263

Table 2 shows the data comparison before and after the repair of the hole model with MeshLab software.

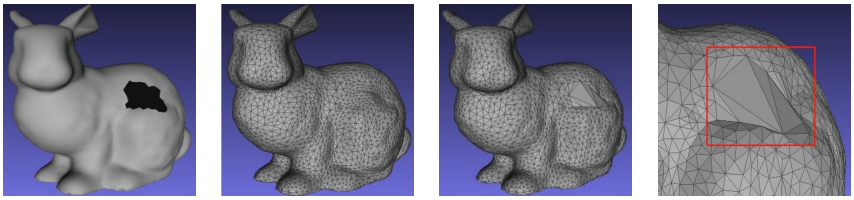

(a) (b) (c) (d)

Figure 11 rocker Model (a)Model with Holes; (b)Repair Result using the Proposed Algorithm; (c)Repair Result using MeshLab; (d)Enlarged View of Repair Mesh using MeshLab;

In terms of the treatment of holes with MeshLab software, it can be seen that MeshLab software only triangulates the hole polygon and does not add new points. Only a simple repair is performed. The repaired mesh not only differs greatly from the initial mesh density of the model but also cannot restore the original curvature.

Table 2 Data Comparison Before and After Repair of the Hole Model Using MeshLab Software

Model name	Number of triangles (front)	Number of triangles (back)	Number of added triangles	Number of vertices (front)	Number of vertices (back)	Number of added vertices	Number of boundary edges
bunny	8546	8574	28	4289	4289	0	36
rocker	18686	18718	32	9359	9359	0	34
horse	96764	96802	38	48403	48403	0	40
blobby	3854	3892	38	1948	1948	0	40

3.2 Function Comparison of the algorithm of the paper and the repaired hole of the CGAL library

CGAL (Computational Geometry Algorithms Library) is a geometric algorithm library developed based on C++ language and is widely used in the geometric calculation-related fields. The authority provides a case of model hole repair. The effect of using this case to repair the above models is shown in Figures 14, 15, 16

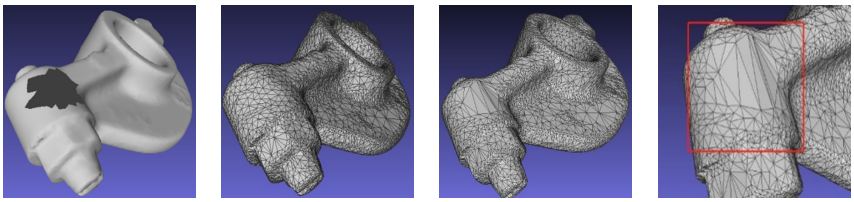

(a) (b) (c) (d)

Figure 12 rocker Model (a)Model with Holes; (b)Repair Result using the Proposed Algorithm; (c)Repair Result using MeshLab; (d)Enlarged View of Repair Mesh using MeshLab;

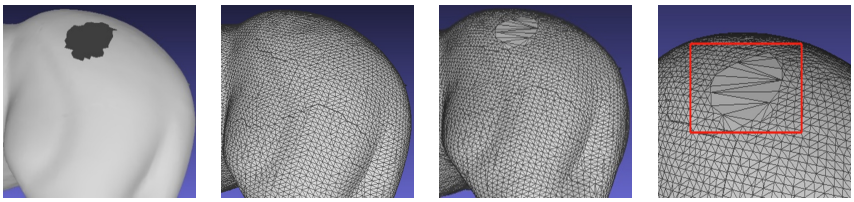

(a) Model with Holes (b) (c) (d)

Figure 13 horse Model (a)Model with Holes; (b)Repair Result using the Proposed Algorithm; (c)Repair Result using MeshLab; (d)Enlarged View of Repair Mesh using MeshLab;

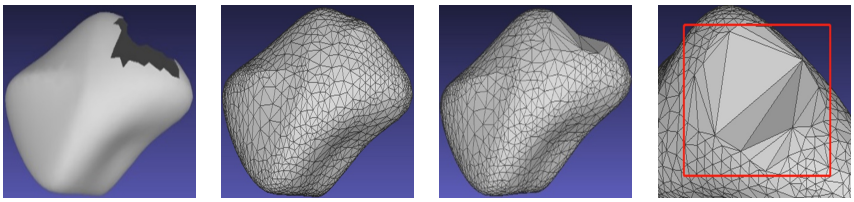

(a) (b) (c) (d)

Figure 14 blobby Model (a)Model with Holes; (b)Repair Result using the Proposed Algorithm; (c)Repair Result using MeshLab; (d)Enlarged View of Repair Mesh using MeshLab;

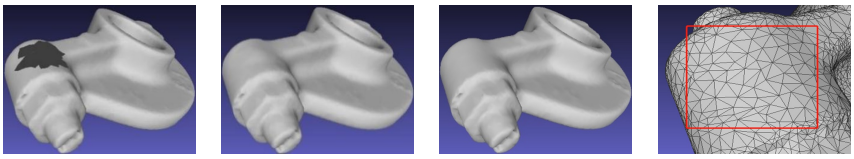

(a) (b) (c) (d)

Figure 15 rocker Model (a)Model with Holes; (b)Repair Result using the Proposed Algorithm; (c)Repair Result using CGAL; (d)Enlarged View of Repair Mesh using CGAL;

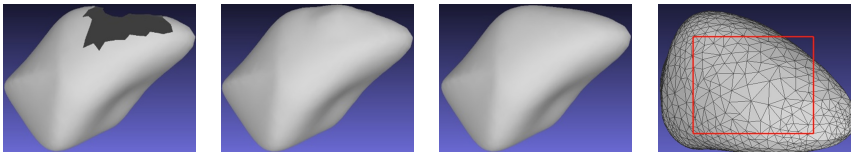

(a) (b) (c) (d)

Figure 16 blobby Model (a)Model with Holes; (b)Repair Result using the Proposed Algorithm; (c)Repair Result using CGAL; (d)Enlarged View of Repair Mesh using CGAL;

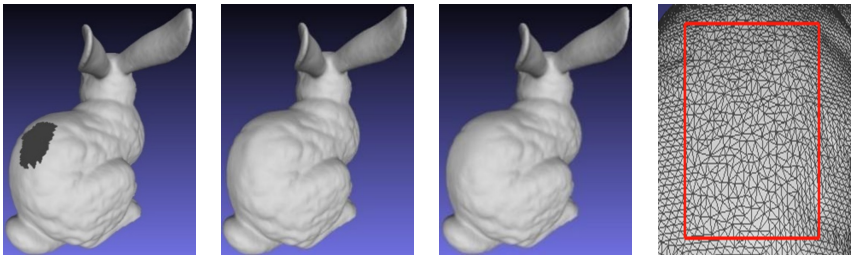

(a) (b) (c) (d)

Figure 17 bunny Model (a)Model with Holes; (b)Repair Result using the Proposed Algorithm; (c)Repair Result using CGAL; (d)Enlarged View of Repair Mesh using CGAL;

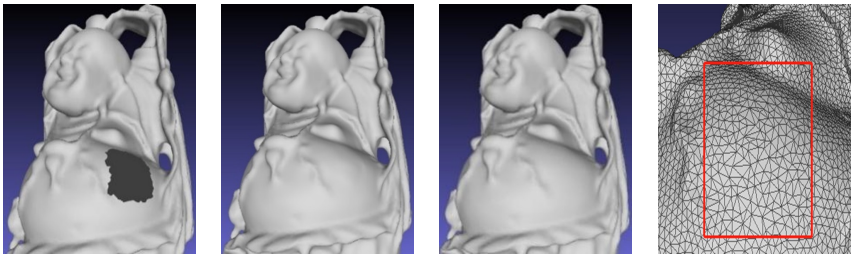

(a) (b) (c) (d)

Figure 18 bunny Model (a)Model with Holes; (b)Repair Result using the Proposed Algorithm; (c)Repair Result using CGAL; (d)Enlarged View of Repair Mesh using CGAL;

and 17. It can be seen that the CGAL library is powerful and the hole repair effect is very ideal. The repaired mesh will also be refined and smoothed. It not only has the same density as the original model but also can accurately restore the lost geometric features. Besides, it has a smooth transition with the original model but the whole repair process consumes a lot of time. In particular, model documents with large documents are very slow to read and very slow to repair. Compared with CGAL, the repair effect on the curved surface of the algorithm of the paper is close and the time consumption is much less. Under the repair mesh with almost the same effect, the algorithm in the paper is more efficient than CGAL.

Table 3 Data Comparison Before and After Repair of the Hole Model Using the CGAL Official Case

Model name	Number of triangles (front)	Number of triangles (back)	Number of added triangles	Number of vertices (front)	Number of vertices (back)	Number of added vertices	Number of boundary edges	Running time of CGAL(s)	Running time of the proposed algorithm(s)
rocker	18686	18790	104	9359	9395	36	36	89.7948	5.307
blobby	3854	4048	194	1948	2011	63	34	35.5048	2.263
bunny	70166	70382	216	35104	35193	89	112	3419.58	2.536
buddh	122760	122978	447	61383	61473	190	69	3516.38	4.398

4 Conclusions

Through the analysis of the above experimental results, the following conclusions can be drawn: the improved wavefront method is used to repair the holes in the paper. When repairing the holes on the curved surface, it can quickly gather into the holes through the geometric space information of the vertex of the hole boundary points, which can repair the holes quickly while avoiding the situation of incomplete holes caused by side repair. A high-quality closed mesh with uniform density is generated, which matches the density of the original model. The hole repair mesh maintains good consistency with the surrounding surface and can almost restore the original surface features of the hole while retaining the original information of the model. The repair operation is convenient and the operation is efficient. The robustness is good. However, for the large hole area, the center part of the repaired mesh is slightly raised, so the regenerated mesh does not look smooth enough.

The time complexity of the algorithm used in the paper is estimated as $O(n^2)$ while the time complexity of the traditional triangulation algorithm is $O(n^3)$. It can be seen that the algorithm in the paper has greatly optimized the speed of mesh repair. Because the difference between α and β has an impact on the effect of generating the repair mesh, the overlapping of triangle patches may appear in the obtained repair mesh. Detail treatment, such as checking whether the position is reasonable each time a triangle surface is added to avoid the occurrence of narrow triangles and mesh intersection. These treatments will affect the quality and beauty of the generated mesh.

Acknowledgements
The authors thank the editor and anonymous reviewers for their helpful comments and valuable suggestions. I would like to acknowledge all our team members.

Funding
This research was supported by the Major Scientific Research Project for Universities of Guangdong Province (No.2019KTSCX260, 2019KZDXM015, 2020ZDZX3058)

Abbreviations
Central Processing Unit (CPU)
Computational Geometry Algorithms Library(CGAL)

Availability of data and materials
Text for this section. . .

Declarations
Ethical Approval and Consent to participate: Approved.
Consent for publication: Approved.
Availability of supporting data: We can provide the data.

Competing interests
There are no potential competing interests in our paper. And all authors have seen the manuscript and approved to submit it to your journal. We confirm that the content of the manuscript has not been published or submitted for publication elsewhere.

Authors' contributions
All authors take part in the discussion of the work described in this paper. These authors contributed equally to this work and should be considered co-first authors.

Authors' information
Jing Huang, born in 1967, female, Professor. Her main research interests are computer graphics and image technology, virtual reality technology, etc. E-mail: huangjing@139.com.
Weicong Li, born in 1998, male, graduate student. His main research interests are computer graphics and image technology and virtual reality technology. E-mail: congcongcba@163.com.
Mengjie Ye received the Ph.D. degree from Macau University of Science and Technology in 2013. He worked as a Postdoctoral Researcher at the Institute of Space Science of Macau University of Science and Technology and a distinguished Associate Researcher at Sun Yat-sen University. He is currently a lecturer with the School of Information Technology, Beijing Normal University, Zhuhai. His research interests include computer graphics, machine vision, and remote sensing data processing.

Author details
Research Center for Intelligent Engineering and Educational Application, Beijing Normal University at Zhuhai, Zhuhai, China.

References
1. Cui, L., Zhang, G., Wang, J.: Hole repairing algorithm for 3d point cloud model of symmetrical objects grasped by the manipulator. Sensors **21**(22), 7558 (2021)
2. Feng, C., Liang, J., Ren, M.: A fast hole-filling method for triangular mesh in additive repair. Applied Sciences **10**(3), 969 (2020)
3. Quinsat, Y.: Filling holes in digitized point cloud using a morphing-based approach to preserve volume characteristics. The International Journal of Advanced Manufacturing Technology **81**(1), 411–421 (2015)
4. Centin, M., Pezzotti, N., Signoroni, A.: Poisson-driven seamless completion of triangular meshes. Computer Aided Geometric Design **35**, 42–55 (2015)
5. Mineo, C., Pierce, S.G., Summan, R.: Novel algorithms for 3d surface point cloud boundary detection and edge reconstruction. Computer Aided Geometric Design **6**(1), 81–91 (2019)
6. Davis, J., Marschner, S.R., Garr, M.: Filling holes in complex surfaces using volumetric diffusion. In: IEEE (ed.) First International Symposium on 3D Data Processing Visualization and Transmission, pp. 428–441 (2002)
7. Ju, T.: Robust repair of polygonal models. ACM Transactions on Graphics **23**(3), 888–895 (2004)
8. Hétroy, F., Rey, S., Andujar, C.: Mesh repair with user-friendly topology control. Computer Aided Design **43**(1), 101–113 (2004)
9. Zhang, L., Pan, X., An, X.: A smooth filling algorithm for triangle mesh surfaces. Journal of Engineering Graphics **4**, 113–119 (2002)
10. Wang, X., Cao, J., Liu, X.: Advancing front method in triangular meshes hole-filling application. Journal of Computer Aided Design and Computer Graphics **23**(6), 1048–1054 (2011)
11. Ji, D.: Hole repairing in triangular meshes based on radial basis function. Journal of Computer Aided Design and Computer Graphics **17**(9), 1976 (2005)
12. Xie, Q., Geng, G.: Research on hole-filling algorithm for 3d models. Application Research of Computers **30**(10), 3175–3177 (2013)
13. Liepa, P.: Filling holes in meshes. In: Proceedings of the 2003 Eurographics/ACM SIGGRAPH Symposium on Geometry Processing, pp. 200–205 (2003)
14. Lu, F.: Research on hole-filling algorithm on meshes for digitalization of cultural relic. PhD thesis, Wuhan University of Technology (2018)
15. Lohner, R., Parikh, P., Gumbert, C.: Interactive generation of unstructured grids for three-dimensional problems. In: Conference on Numerical Grid Generation in Computational Fluid Mechanics, pp. 687–697 (1988)
16. Lo, S.H.: Volume discretization into tetrahedra—i. verification and orientation of boundary surfaces. Computers & Structures **39**(5), 493–500 (1991)
17. Li, Y., Geng, G., Wei, X.: A smooth filling algorithm for triangle mesh surfaces. Computer Engineering **43**(10), 209–215221 (2017)
18. Liu, S., Liang, J., Dong, B.: Rapid mesh hole filling in body model. Journal of Xi'an Jiaotong University **52**(08), 37–42 (2018)